CONSTRAINED VARIANCE CONTROL OF PEAK PRESSURE POSITION BY SPARK IONIZATION FEEDBACK

N. Rivara, [1] **P. Dickinson, A. T. Shenton** [2]

Powertrain Control Group, Department of Engineering,
The University of Liverpool, Liverpool, L69 3GH, U.K.

Abstract:
A neural-network (NN) based scheme is presented for control of cylinder peak pressure position (PPP) by spark ignition (SI) timing in a gasoline internal combustion (IC) engine. Spark-ionization current from the spark plug is used to act as a virtual PPP sensor. Off-line training using principal component analysis (PCA) data predicts the cylinder peak pressure position under varying engine load, speed and spark advance (SA) settings. Results demonstrate that the PPP prediction of the NN correlates well with those measured from in-cylinder pressure sensors. A constrained-variance (CV) controller, which is a robust form of minimum-variance (MV) controller, is designed and applied to regulate the PPP by SA control action. This is validated by experimental implementation on a port fuel-injected (PFI) 4-cylinder 1.6l gasoline internal combustion (IC) engine.

Keywords: Spark Ionization Neural Network, Ignition Timing, Feedback Control, Principal Component Analysis, Minimum Variance, PPP control

1. INTRODUCTION

Currently SI timing strategies are mapped into the electronic control unit (ECU) with experimentally predetermined settings in feedforward look-up tables and operate through open loop control. There is extensive time and effort in the calibration procedure for the spark map which is required to cover all possible operating points. Alternatively the use of in-cylinder pressure as a feedback control variable removes the requirement for this laborious task. Further advantages to this feedback approach are obtained by the disturbance rejection properties including automatic compensation for varying environmental conditions, engine wear and fuel characteristics, and the potential for reduced lean-limit operation by reduction of cycle-to-cycle combustion variation (CCV). To-date, however their use in production automotive engines has so far been prevented by the prohibitive cost of suitable pressure sensors.

Variability occurs in the cycle to cycle combustion process within a SI combustion engine cylinder through the alteration of key parameters such as SI timing and through the natural inconsistency of turbulent flame propagation. Hence the CCV when spark timing is fixed is indicated as noise in the PPP output (Triantos, 2006). This variability in the PPP may be determined directly and so can be used in feedback control since it is a highly useful measure of CCV of combustion. Adjusting SI timing directly affects the combustion initiation process and will thus alter the PPP and affect the amount of torque output that can be achieved whilst minimizing losses. For maximum

[1] This work was supported in part by the EPSRC (Engineering and Physical Science Research Council).
[2] Email: shenton@liv.ac.uk

best torque (MBT) the optimal PPP depends on the particular engine configuration but is typically around 16° after top dead centre (ATDC) (Heywood, 1988).

A low cost, non-intrusive manner of obtaining the in-cylinder pressure information is by spark ionization. By applying a DC bias voltage across a spark-plug, the resulting electrical current between the two electrodes of the spark-plug during combustion can be measured and relates to the pressure in the cylinder.

The spark ionization signal has been used in production vehicles so far exclusively for misfire detection, an event that produces no ionization of the air/fuel mixture within the cylinder, and knock detection, (Wang and Zhou, 2003; Zhu et al., 2005). The use of a spark ionization signal for feedback control of the SA has also been investigated and attempts to interpret the signal and identify the PPP include Eriksson et al. (1996); Asano et al. (1998); Hellring et al. (1999b); Holmberg and Hellring (2003); Wickstrom et al. (1998); Zhao and Ladommatos (1997).

Figure 1 displays the location of these peaks for a typical, single spark ionization signal and the actual in-cylinder pressure. The occurance and detection of the 'second peak' in the spark ionization signal is fundamental to identifying the correlation between PPP and the spark ionization signal. Although the maximum of the 'second peak' appears to occur at the PPP, though there is variance due to stochastic nature of the process.

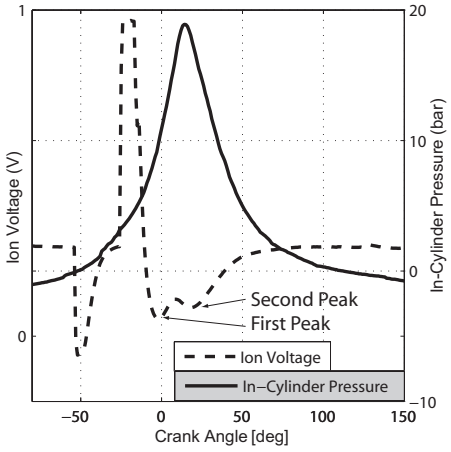

Fig. 1. Actual cylinder pressure and a typical spark ionization current signal from a non-averaged combustion cycle

Early work proposed that the 'pressure indicating' section of the spark ionization signal has a shape close to Gaussian curve functions (Eriksson et al., 1996). This Gaussian curve model is fitted to the measured ionization current in the least-squares sense. However the ionization signal varies under different operating conditions, load, etc, and a simple Gaussian function cannot fit sufficiently well.

Subsequent work involved processing of the pressure related section of the spark ionization curve with principal component analysis (PCA). These principal components are then used as inputs for a NN which is trained to relate the PCA values to a peak pressure position (Wickstrom et al., 1998; Hellring et al., 1999b).

Although prediction of PPP using the spark ionization signal has been researched (Zhu et al., 2004, 2005; Eriksson and Neilsen, 1997), there is little evidence of closed loop control using the spark ionization signal and NNs being implemented and validated on an engine for real-time control.

Many of the results presented in literature is research use a 'hold-out' data set (a portion of the same original sampled dataset from which the training dataset is also taken)(Holmberg and Hellring, 2003; Hellring et al., 1999a; Gazis et al., 2006; Hanzevack et al., 1997). This implies difficulties in proving the NN online.

This work investigates PPP regulation controlled using SI timing by a constrained variance feedback control technique employing a NN to predict PPP from various engine signals; air bleed valve (ABV), manifold absolute pressure (MAP) and the spark ionization signal.

2. EXPERIMENTAL SET-UP

The experimental engine used is a SI , Ford Zetec 1.6l, 16 valve, four-stroke, four-cylinder, double overhead cam, multi-point fuel injected IC engine. A Ford production EECIV ECU controls the fuel whilst spark advance (SA) and ABV were controlled externally. The spark ionization system was built in-house and implemented onto cylinder 4. Actual in-cylinder pressure is measured through Kistler^{TM} Piezo-electric pressure transducers and charge amplifiers. Load is applied to the engine crankshaft through a low inertia dynanometer. An optical encoder is mounted directly to the crankshaft and sampling of all sensor signals can occur once per degree of crankshaft rotation though PPP is calculated as a single data point per engine cycle, along with engine speed and integrated MAP.

3. SPARK IONIZATION SIGNAL PROCESSING

PCA is a multivariate statistical process that can obtain the most significant characteristics in the

data set and thus be used to reduce sample data sizes. A new set of variables, the 'principal components', is generated from an original data set which is as large but it is commonplace for the sum of the variances of the first few principal components to have a substantial amount of the total variance of the original data. Hence the original data set will often be effectively represented by the few most 'principal' component scores (Johnson and Wichern, 1982; Haykin, 1999).

A specific window of the spark ionization signal, which is believed to contain information relating to the PPP is calculated to be the 30° of crank angle, between 25° and 55° after the spark event. The top 5 principle components were selected as these contained over 99.9% of the total signal variance.

3.1 Artificial Neural Network

A neural network size was chosen by a reduction technique, whereby an initial large network achieves a theoretical minimum squared error (MSE). Reducing network neurons and layers and evaluating MSE is done systematically until the minimum network size with acceptable MSE is achieved. Figure 2 shows the chosen 2 layer Non-Linear AutoRegressive with eXogeneous input (NARX) network where the input layer weight matrix is denoted IW and other layer weight matrices are denoted LW. f_1 activation function is tansigmoid functions while f_2 is a pure linear activation function. Layer 1 contains 10 neurons whilst layer 2 contains 1 neuron. The network has a single feedback loop from final layer to the first layer through a tapped delay line (TDL) to instigate the delays present in the data; $y(t-1), y(t-2)$. The 7 inputs pass through a specific TDL where the output of this is a vector made up of the input signals at the current time and the previous input signals; $u(t), u(t-1)$. The bias values for each layer are denoted $b_1, \ldots, b_3$, k is algebraically the number of neurons per layer and R represents the number of input vectors at time (t), in this case $R = 7$. The defining equation of

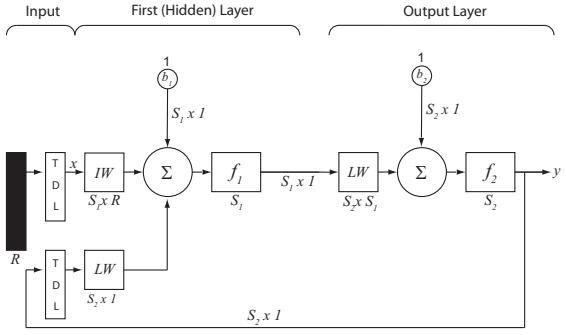

Fig. 2. Schematic of a two layer NARX network

Table 1. Perturbed signals for the use of training a neural network

Signal	Range	Perturbation Frequency
ABV [$\%_{duty}$]	54 to 62	0.7 seconds
Load [V]	-0.18 to -0.22	0.8 seconds
SA	20° to 34° BTDC	0.4 seconds

this NARX network is the difference equation

$$y(t) = f(y(t-1), y(t-2), u(t), u(t-1))$$

3.1.1. Network Training The identification of the relationship between the 'window' of data of the spark ionization curve and the PPP is the purpose of the NN employed in the application.

Perturbed input signals are excited simultaneously by scaled, biased uniform random numbers over a range to obtain dynamic network training data, as indicated in the table 1. The excitation signals perturb the engine speed between 1000rpm to 1600rpm whilst the integrated MAP fluctuates between 75 and 110 bar[2]. 3000 combustion cycles are acquired and split equally into three parts; 1000 cycles for network training, 1000 cycles for validation of the NN and the final 1000 cycles as a 'hold-out' data set for offline proving before engine implementation occurs. 5 rows of 1000 cycles obtained from PCA representing the spark ionization signal are used as input training data along with integrated MAP signal[3] (used as an indication of load) and the engine speed. The corresponding PPP measured from the in-cylinder pressure sensors obtained over the 1000 cycles are the output training data. Mean values are removed and the data normalised according to NN theory for training rapidness and network adaptivity ease (Haykin, 1999).

'Bayesian-Regulation backpropagation with early stopping' is employed to train the network, which prevents overtraining. The validation dataset is presented to the network after each training epoch; early stopping occurs when the MSE of the validation dataset increases.

4. NEURAL NETWORK PROVING

After offline training, the 'hold-out' dataset is used to prove the network is predicting the PPP accurately. To quantify the accuracy of the NN predictions on this 'hold-out' dataset, two measures of performance are used; Normalised Mean Square Error (NMSE) and R^2, which is the coefficient of determination where 1 is a maximum. Over the 1000 cycles of 'holdout' data, $NMSE = 0.0137$ and $R^2 = 0.8029$ indicating over 80% of

[3] Integrated over 180° prior to sampling

the variance in the PPP is explained by the estimated PPP based on the ionization signal. Good

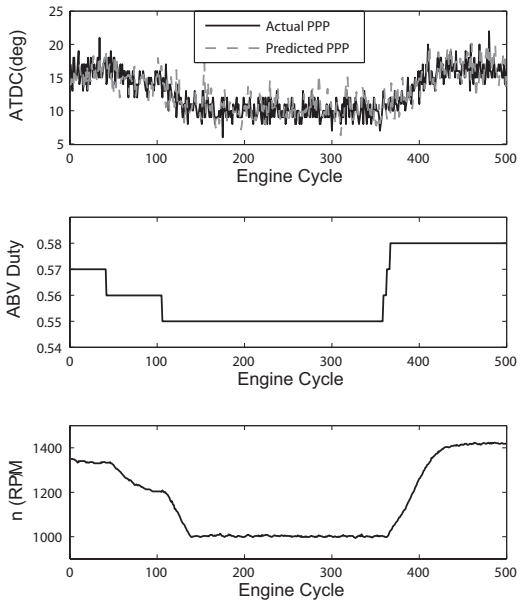

Fig. 3. Correlation of predicted PPP and actual PPP over 500 cycles due to step changes in ABV

accuracy of the NN at predicting PPP is implied by the correlation of 'hold-out' data. This was followed by implementation onto the engine to predict PPP in real time whereby engine variables were brought in line with the ranges used for identification data acquisition and ABV, load and SI timing were step-changed individually. A visual on-line measurement of actual PPP was done simultaneously with the Kistler pressure sensor. Accuracy of the NN is presented in figures 3, 4 and 5.

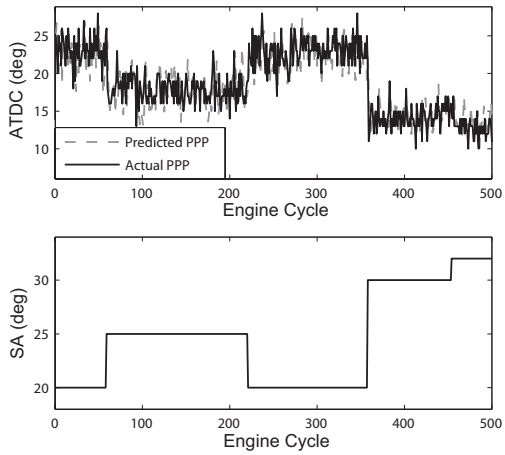

Fig. 4. Correlation of predicted PPP and actual PPP over 500 cycles due to step changes in spark ignition Timing

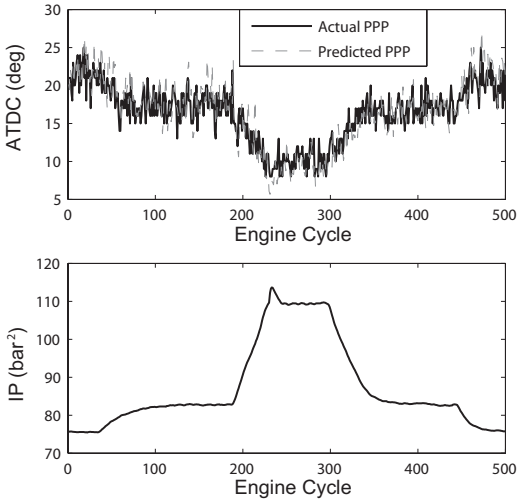

Fig. 5. Correlation of Predicted PPP and Actual PPP over 500 cycles due to step changes in Applied Load

5. CONTROL TECHNIQUES

The good correlation of actual PPP to predicted PPP indicates a successful NN. A desired PPP set-point of 16° for MBT is suggested and a feedback scheme to maintain this, which controls the SA accordingly uses this signal. The feedback scheme should be of a minimum variance type since the PPP signal is affected by combustion variability, stochastic flame propagation and sensor noise (Triantos, 2006).

The feedback controller was designed using a linear model identified at the mean operating range of the NN estimator by perturbing the SA and monitoring the PPP from the virtual sensor, with load and ABV fixed at their respective mean values. A SISO linear Auto Regressive and Moving Average eXogenous (ARMAX) model was obtained by perturbing the SA and measuring the predicted PPP. The load and ABV were fixed around the mid-point of the intended NN operating range. A summary of the excitation signals is detailed in table 2. The ARMAX model may be represented as

$$y(t) = \frac{B(q)}{A(q)}u(t) + \frac{C(q)}{A(q)}e(t) \quad (1)$$

The identified parameters lead to the following transfer functions

$$G_b(z) = \frac{B(z)}{A(z)} = \frac{b_1 z^{-1} + b_0 z^{-2}}{a_2 + a_1 z^{-1} + a_0 z^{-2}}u(t) = \frac{-0.7144z^{-1} + 0.006716z^{-2}}{1 + 0.00792z^{-1} - 0.1281z^{-2}}u(t) \quad (2)$$

$$G_c(z) = \frac{C(z)}{A(z)} = \frac{c_2 z + c_1 z^{-1} + c_0 z^{-2}}{a_2 + a_1 z^{-1} + a_0 z^{-2}}e(t) = \frac{1 + 0.1316z^{-1}}{1 + 0.00792z^{-1} - 0.1281z^{-2}}e(t) \quad (3)$$

A constrained variance (CV) controller was designed and evaluated for suitability to the problem to achieve a good compromise between tracking and low output variance, and was applied and

Table 2. Perturbed signals used to generate ARMAX model of estimated PPP

Signal	Range	Perturbation Frequency
ABV [$\%_{duty}$]	Steady state 0.58/1	N/A
Load [V]	Steady state - 0.18	N/A
SA Timing	20° to 34° BTDC	0.4 seconds

evaluated in simulation using the determined ARMAX model. A negative feedback control scheme, as illustrated in figure 6, was used with the resulting controller where G_c represents the colouring filter transfer function, G_b being the plant model, K the controller where w denotes the disturbance input of unit variance white noise. For the closed

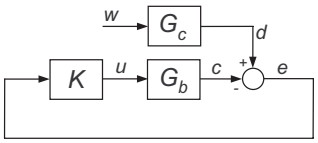

Fig. 6. Implemented Closed Loop Feedback Control

loop system the transmission from the noise input w to the output error e is given by

$$G_w^e(z) = \frac{e(z)}{w(z)} = \frac{G_c(z)}{1 + K(z)G_b(z)} \tag{4}$$

The output variance σ_e^2 for a system of (4) is given (see Lindorff (1965)) as:

$$\sigma_e^2 = \frac{1}{2\pi j} \oint_{c1} G_w^e(z^{-1}) G_w^e(z) \frac{dz}{z} \tag{5}$$

where $c1$ is the contour of the unit circle. Since the controller is required to provide tracking a proportional-integral (PI) controller $\frac{(k_p+k_i)z-kp}{z-1}$ is considered. For the system of Eqn. (1), the closed loop transfer function of Eqn. (4) can be expressed as

$$G_w^e(z) = \frac{(c_2z^2 + c_1z + c_0)(z-1)}{(a_2z^2 + a_1z + a_0)(z-1) + ((k_p + k_i)z - k_p)(b_1z + b_0)} \tag{6}$$

For a specified output variance, symbolic solutions of k_p and k_i for the definite integral of Eqn. (5) can readily be obtained. Several fixed variance values were trialled in the design of the CV controller to obtain the best trade-off between tracking and output variance. Simulation revealed an output variance of 1.1 deg^2 was sufficient to provide adequate tracking and non-zero mean disturbance rejection whilst retaining a low level of output variance. Accordingly, a symbolic solution for k_i and k_p to the definite integral of Eqn. (5) for the closed loop system was obtained and from plotted loci of possible controller gains with the desired output variance, the maximum permitted integral gain was selected to incorporate the tracking requirement resulting in the constrained variance controller (Dickinson, 2007)

$$K(z) = \frac{0.0740z + 0.2833}{z - 1} \tag{7}$$

Table 3. Stability Margins for the Controller

Control	Gain Margin	Phase Margin
CV	14.9dB at 26.2rad/s	83.5° at 1.89rad/s

5.1 Validation of feedback scheme

The robustness of the controller was evaluated and the gain and phase margin are detailed in table 3.

The CV type controller was implemented with the NN system in a feedback loop for control of PPP. Through step changes in the ABV signal and by varying the applied load through the dynamometer, robustness of the controller was examined. The closed loop system was well behaved over a range within the ARMAX models identification data range. The system, through step input signal disturbances was able to track to a desired PPP value as illustrated in Fig. 7 where the mean of predicted PPP matches the PPP tracking demand. Figure 8 illustrates the predicted

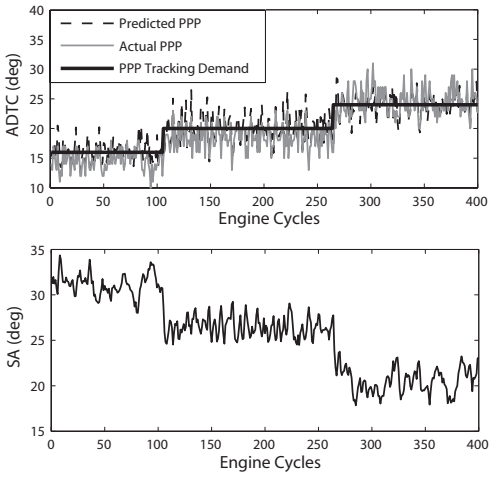

Fig. 7. Predicted PPP and actual PPP tracking to demanded PPP and required SA

PPP tracking to a demanded PPP whilst step disturbances are applied to the ABV, thus altering engine speed. Figure 9 illustrates the predicted PPP tracking to a demanded PPP of 16° ATDC whilst step disturbances are applied to the load, thus altering engine speed and MAP.

The difficulties in modelling such a system are highlighted with a 30% percent increase observed when considering the controlled variance of the predicted PPP. This is significantly higher than the variance increase in simulation (10%). Furthermore, the validity of the model reduces when changing the operating point away from the identified region. For effective control over the entire operating region of the PPP estimation algorithm it is suggested a series scheduled linear CV controllers should be considered.

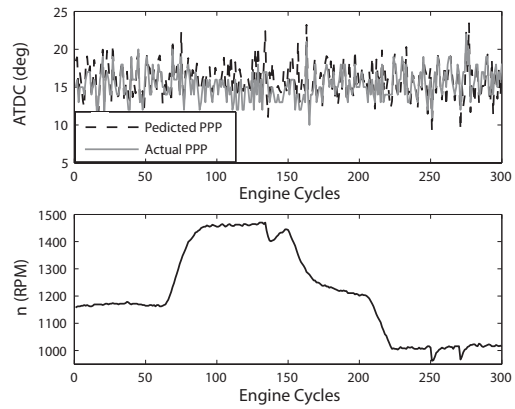

Fig. 8. Predicted PPP and measured PPP tracking to demanded PPP with step disturbances to ABV

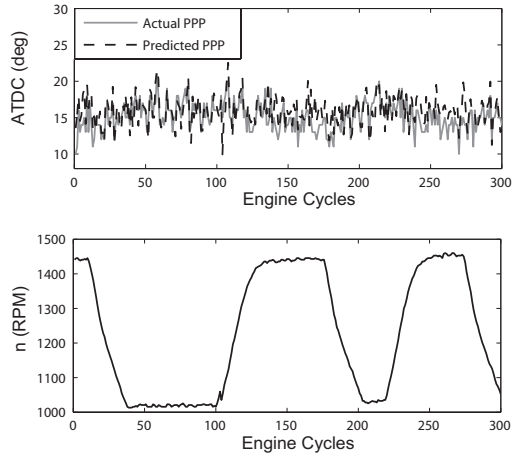

Fig. 9. Predicted PPP and actual PPP tracking to demanded PPP with step disturbances to Load

6. CONCLUSIONS

This research demonstrates that through the use of the spark ionization signal, a NN and the implementation of a constrained variance control technique, the PPP can be predicted and controlled over the range of an identified model for a single cylinder. The system is demonstrated to be robust to step disturbances of load and speed when applied to an engine in real-time, and successfully tracks to a desired PPP setting.

REFERENCES

M Asano, T Kuma, M Kajitani, and M Takeuchi. Development of new ion current combustion control system. *SAE*, (980162), 1998.

P B Dickinson. *Robust Low-Order Control Techniques with Powertrain Applications*. PhD Thesis, University of Liverpool, 2007.

L Eriksson and L Neilsen. Closed loop ignition control by ionization current interpretation. *SAE*, (970854), 1997.

L Eriksson, L Nielsen, and J Nytomt. Ignition control by ionization current interpretation. *SAE*, (960045), 1996.

A Gazis, D Panousakis, R Chen, and W-H Chen. Computationally inexpensive methods of ion current signal manipulation for predicting the characteristics of engine in-cylinder pressure. *IMechE, Journal of Engine Research*, 7, 2006.

E L Hanzevack, T W Long, C M Atkinson, and M L Traver. Virtual sensors for spark ignition engines using neural networks. *Proceedings of the American Control Conference*, (0-7803-3832-4/97), 1997.

S Haykin. *Neural Networks, A Comprehensive Foundation*. Prentice-Hall, 1999.

M Hellring, T Munther, T Rognvaldsson, N Wickstrom, C Carlsson, M Larsson, and J Nytomt. Robust afr estimation using the ion current and neural networks. *SAE*, (1999-01-1161), 1999a.

M Hellring, T Munther, T Rognvaldsson, T Wickstrom, C Carlsson, M Larsson, and J Nytom. Spark advance control using the ion current and neural soft sensors. *SAE*, (1999-01-1162), 1999b.

J Heywood. *Internal Combustion Engine Fundamentals*. McGraw-Hill, 1988.

U Holmberg and M Hellring. A simple virtual sensor for combustion timing. *Journal of Dynamics, Measurement and Control*, 125:462–467, 2003.

R A Johnson and D W Wichern. *Applied Multivariate Statistical Analysis*. Prentice-Hall, 1982.

D P Lindorff. *Theory of Sampled-Data Control Systems*. Wiley, 1965.

G Triantos. *NARMAX Modelling and Control With Powertrain Applications*. PhD Thesis, University of Liverpool, 2006.

Y Wang and L Zhou. Investigation of the detection of knock and misfire of a spark ignition engine with the ionic current method. *IMechE*, 271(D:J):617–621, 2003.

N Wickstrom, M Taveniku, A Linde, M Larsson, and B Svensson. Estimating pressure peak position and air-fuel ratio using the ionization current and artificial neural networks. *IEEE*, (0-7803-4269-0):972–977, 1998.

H Zhao and N Ladommatos. Engine performance monitoring using spark plug voltage analysis. *IMechE*, 211:499–509, 1997.

G Zhu, I Haskara, and J Winkelman. Stochastic limit control and its application to knock limit control using ionization feedback. *SAE*, (2005-01-0018), 2005.

G G Zhu, C F Daniels, and J Winkelman. Mbt timing detection and its closed-loop control using in-cylinder ionization signal. *SAE*, (2004-01-2976), 2004.